https://doi.org/10.5194/egusphere-2025-1372
Preprint. Discussion started: 8 April 2025

Heterogeneity of the horizontal environment drives community assemblages and species coexistence of prokaryotic communities in cold seep sediments

Qixuan Wu[a], Jingchun Feng[a,b,*], Yongji Huang[a,b,c,d], Song Zhong[a], Cun Li[a,b,c,d], Si Zhang[a,b,d]

[a] Guangdong Basic Research Center of Excellence for Ecological Security and Green Development, Guangdong University of Technology, Guangzhou 510006, China

[b] Southern Marine Science and Engineering Guangdong Laboratory (Guangzhou), Guangzhou, 511458, P. R. China

[c] University of Chinese Academy of Sciences, Beijing 100049, China

[d] South China Sea Institute of Oceanology, Chinese Academy of Sciences, Guangzhou 510301, P. R. China

[*]Corresponding author. E-mail address: fengjc@gdut.edu.cn. (J. C. Feng)

Tel: +86-20-39322141. Fax: 020-39322141

https://doi.org/10.5194/egusphere-2025-1372
Preprint. Discussion started: 8 April 2025

HIGHLIGHTS:

1. Habitat heterogeneity affected the species coexistence and community assembly.
2. CH_4 was the key driving factor of prokaryotic community diversity and assembly.
3. The assembly of prokaryotic communities were mainly stochastic processes.
4. Bacteria and archaea showed different coexistence patterns in seepage area.

GRAPHICAL ABSTRACT:

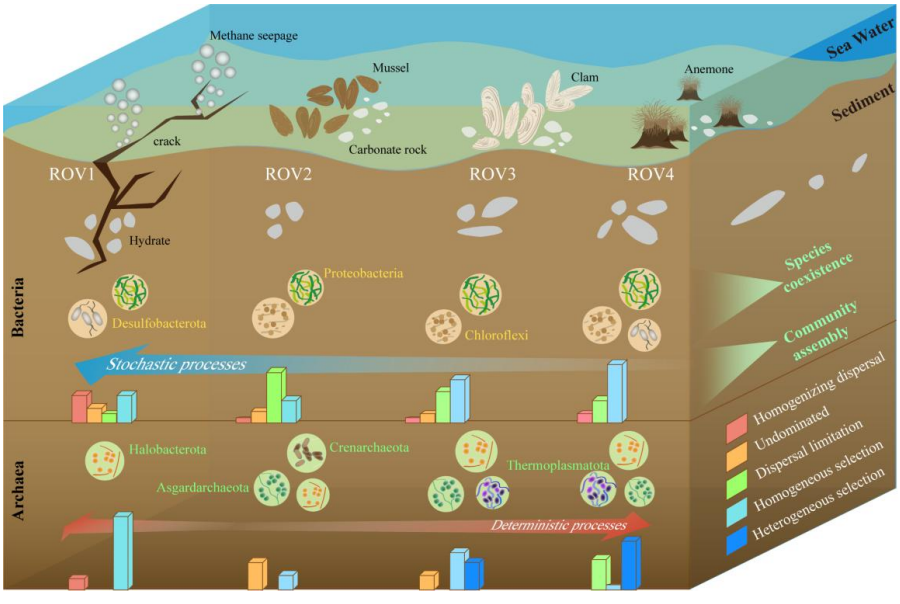

https://doi.org/10.5194/egusphere-2025-1372
Preprint. Discussion started: 8 April 2025

ABSTRACT

Microbes in cold seep sediments play important roles in controlling methane filtration and the global geochemical cycle, but little is known about microbial distribution and community assembly in the horizontal sediment profile. This study conducted a comprehensive investigation of prokaryotic community diversity in sediments from different habitats in a cold seep ecosystem of the South China Sea. Compared to other sites, the prokaryotic community in the methane seep site showed a lower α-diversity. Halobacterota was dominant in methane seep site, while higher abundances of Chloroflexi and Asgardarchaeota were observed in the fauna sites. The assembly process of the bacterial community in the methane seep site was mainly a stochastic process, while the archaeal community was mainly formed by a deterministic process. The prokaryotic community in fauna sites was influenced by both stochastic and deterministic processes. The heterogeneity of the horizontal environment such as the content of CH_4, Ba^{2+}, total inorganic carbon, and SO_4^{2-} influenced prokaryotic community diversity and drove the community assembly processes. Additionally, bacterial species coexisted more closely in methane seep site than in other sites, but archaea did the opposite. Overall, this study revealed how prokaryotes build communities in different cold seep habitats.

Keywords: Cold seep sediment, Horizontal environmental heterogeneity, Community diversity, Community assembly, Species coexistence

https://doi.org/10.5194/egusphere-2025-1372
Preprint. Discussion started: 8 April 2025

1. Introduction

Cold seeps are deep-sea phenomena caused by fluids rich in methane, hydrogen sulfide, and other hydrocarbons released from seabed sediments (Feng et al., 2018; Lee et al., 2014). In this type of seepage environment, the oxidation of methane is mainly carried out by sulfate-driven anaerobic oxidation of methane, which is dominated by methanotrophic archaea and sulfate-reducing bacteria (SRB) (Lin et al., 2022). With the consumption of methane and sulfate, this biochemical process releases abundant dissolved bicarbonate and hydrogen sulfide (Gong et al., 2023; Lin et al., 2022). These processes provide carbon and energy sources for the surrounding prokaryotic and macrofaunal communities, derived from the thriving cold seep chemosynthetic ecosystem (Lyu et al., 2023).

During ecological succession at a cold seep, crevices appear in the sediments as a result of methane seepage in the early stage; this continuous seepage of methane attracts microorganisms capable of metabolizing methane to colonize the site. An abundance of faunal organisms such as deep-sea white clam and sea anemone settle down in the middle stage of the seepage. With the decreasing concentration of methane as one goes away from the seep itself, mussels gradually dominate in the cold seep area, while massive subsidence of carbonate rock often occurs in the later stage (Feng et al., 2023a). The intensity of methane seepage varies in successional periods, resulting in the formation of different habitats. In Haima cold seeps located in the South China Sea as described below, remotely operated vehicle observations have confirmed the presence

https://doi.org/10.5194/egusphere-2025-1372
Preprint. Discussion started: 8 April 2025

of typical cold seep biota including mussels, tubeworms, clams, and microbial mats (Chen et al., 2023; Hu et al., 2019). Different methane seepage rates and densities of various organisms were also observed in different habitats (Xu et al., 2020). Correspondingly, dense populations of mussels, clams, Alvin shrimp, and deep-sea crabs appeared in strongly bubbling areas, while large amounts of carbonate rocks and dead shells existed in the weak seepage zone (Feng et al., 2023b; Liang et al., 2017; Xu et al., 2020). Therefore, the different stages of cold seep succession harbor a variety of habitats, and the horizontal heterogeneity drives the establishment of unique microbial communities within each habitat (Chen et al., 2023; Niu et al., 2023).

Two theories have received a large amount of attention in ecology, namely the niche and neutral theories (Wennekes et al., 2012; Whitfield, 2002). Niche theory advocates that deterministic processes such as environmental filtering, biological interactions, and interspecific trade-offs induce community composition, abundance, and distribution. The neutral theory argues that species are functionally equal and highly affected by stochastic processes such as colonization, extinction, and speciation (Chase and Myers, 2011; Ning et al., 2020). These ecological processes are summarized as selection, dispersal, speciation or diversification, and ecological drift, which individually or collectively drive the community assembly of a local microbial community. Additionally, when interspecific competition is lower than intraspecific competition and leads to niche differentiation, species begin to coexist (Gravel et al., 2011). The species coexistence of a microbial community can be represented by

https://doi.org/10.5194/egusphere-2025-1372
Preprint. Discussion started: 8 April 2025

ecological co-occurrence networks that use microbial species as nodes and interspecific interactions as links. In the early stage of a cold seep, a methane seep is the dominant phenomenon and the symbiont of anaerobic methanotrophic archaea (ANME) and SRB drive metabolic processes in sediments (Cui et al., 2019). At other stages, microbe-shellfish symbionts appeared in faunal habitats. It has been reported that two thiotrophic, one methanotrophic, and one methylophaga-related symbiont have been found in the deep-sea mussel *Idas* sp., which collectively supported the primary chemosynthesis that involves methane and sulfide (Duperron et al., 2008). Previous studies have shown that methanotrophic and thiotrophic symbionts can be found in small mussels with a increasing ability to collectively provide carbon nutrition to the host during the early stages of growth (Duperron et al., 2011). The species and abundance of symbionts may vary greatly within a host and between different sites, which may be related to different biogeochemical conditions in the habitats of mussels (Duperron et al., 2007).

Although many studies have been conducted on cold seep sediments, these studies have mainly focused on in-situ investigations of the diversity of the microbial community and the related geochemical processes. For example, several studies have shown that methane fluids promote microbial aggregation and evolution in sediments (Dong et al., 2023; Zhong et al., 2023), and cold seep microorganisms play an important role in carbon, sulfur, and nitrogen element cycles (Sun et al., 2020). Methane-induced horizontal environmental heterogeneity may lead to distinct microbial community assembly and a close connection between species (Jiang et al., 2022; Zhai et al., 2022).

https://doi.org/10.5194/egusphere-2025-1372
Preprint. Discussion started: 8 April 2025

However, a lack of a detailed understanding exists related to how horizontal environmental heterogeneity affects community assembly and species coexistence in different cold seep sediments.

In this study, an investigation of the geochemical properties and microbial community diversity of sediments from four habitats in Haima cold seeps in the South China Sea was carried out. Specifically, 16S ribosomal RNA (rRNA) gene amplification sequencing was applied to measure the bacterial and archaeal communities. Null models and co-occurrence networks were used to characterize the assembly processes and species coexistence patterns of prokaryotic communities. The purposes of this study are to: (i) explore the horizontal distribution of the prokaryotic communities in different cold seep habitats, (ii) clarify community assembly processes and species coexistence patterns along the horizontal scale of cold seep sediments, and (iii) analyze the important environmental factors that drive community diversity, assembly processes and species coexistence.

https://doi.org/10.5194/egusphere-2025-1372
Preprint. Discussion started: 8 April 2025

2. Materials and methods

2.1 Collection of sediment samples and geochemical analysis

The sediments were obtained using a pushcore controlled by a remotely operated vehicle at four sites of Haima cold seeps (16°43′N, 110°28′E) located in the South China Sea during May 2023. Sediment samples at depths of 5, 10, 15, 20, 25, 30, and 35 cm were collected and were stored at −80°C prior to analysis. Of the four sites, the ROV1 site was a methane seep area while the ROV2, ROV3, and ROV4 sites were areas with fauna containing mature mussels, clams, and sea anemones, respectively.

The geochemical parameters measured in the sediment samples included total inorganic carbon (TIC), total organic carbon (TOC), and concentrations of CH_4, SO_4^{2-}, Cl^-, Ba^{2+}, K^+, Ca^{2+}, Mg^{2+}, Fe^{3+}, Cu^{2+}, and Mn^{2+}. Specifically, TIC and TOC were measured by a TOC analyzer (Shimadzu TOC-L, Kyoto, Japan). The CH_4 concentrations were measured by gas chromatography (Trace 1300, Thermo Fisher, Waltham, MA, USA). The concentrations of SO_4^{2-} and Cl^- were detected by ion chromatography (Thermo Fisher AQ-1200). An inductively coupled plasma-optical emission spectrometer (ICP-OES, Thermo Fisher iCAP 7000 series) was used to determine the concentrations of Ca^{2+}, Mg^{2+}, Ba^{2+}, K^+, Fe^{3+}, Cu^{2+}, and Mn^{2+}. All testing procedures follow manufacturer's instructions.

2.2 DNA extraction, PCR amplification, 16s rRNA sequencing

Total genomic DNA was extracted from sediments using a Magnetic Soil And Stool DNA Kit (Tiangen, DP712-02, Tianjin, China). The extracted DNA was qualitied

https://doi.org/10.5194/egusphere-2025-1372
Preprint. Discussion started: 8 April 2025

using qubit fluorometric quantification (Thermo Scientific, Thermo Fisher Scientific Corp.). Using forward primer 341F (5'-CCT ACG GGN GGC WGC AG -3') and reverse primer 806R (5'- GGA CTA CHV GGG TWT CTA AT -3') (Yu et al., 2005) to amplify the V3–V4 region of the bacterial 16S rRNA gene. Archaeal 16S rRNA gene was amplified by forward primer Arc349F (5′-GYG CAS CAG KCG MGA AW-3′) and reverse primer Arc806R (5′-GGA CTA CNS GGG TMT CTA AT-3′) (Takai and Horikoshi, 2000). Six specific bp barcodes were tagged on the primers to distinguish the sequences of each sample in the mixed pools used for Illumina sequencing. Next, PCR amplification was performed using the following settings: pre-denaturation at 95℃ for 3 min, 30 cycles consisting of denaturation at 95℃ for 15 s, annealing at 53℃ for 15 s, and extension at 72℃ for 30 s, and a finally extension at 72℃ for 10 min. The amplified PCR products were purified with DNA Clean Beads (Vazyme, N411-01, China). An equal quantity of DNA from each sample was mixed for amplicon library construction. Amplicon libraries were sequenced on a Novasep-PE250 platform (Illumina Inc., San Diego, CA, USA).

2.3 Data processing and bioinformatics analysis

The bioinformatics tool Quantitative Insights Into Microbial Ecology version 2 (2022.8) was used for data processing. The raw data were split into the amplicon sequences of individual samples by the plugin cutadapt based on each unique barcode. Plugin dada2 was used to complete the quality control of sequences. First, the forward and reverse primers were cut off; then the low-quality sequences and chimeras were

https://doi.org/10.5194/egusphere-2025-1372
Preprint. Discussion started: 8 April 2025

filtered. Next, the high-quality reads with 100% similarity were clustered to form amplicon sequence variants (ASVs), and the feature tables and representative sequences were obtained. To further clarify the representative sequences, the feature-classifier plugin and the Silva reference database (version 138.1) were used to perform taxonomic annotations and produce a taxonomy table. Finally, the phylogenetic trees were constructed using the Phylogeny plugin.

2.4 Statistical analysis

The following data analysis was performed by R software (vers. 4.3.0). The α-diversities of the bacterial and archaeal communities were calculated using the "vegan" package in R, including Chao1 richness, Observed ASVs, Phylogenetic diversity, Shannon diversity and Goods coverage. Furthermore, the least significant difference method was used (using the "agricolae" package) to calculate the significant differences between samples (Meier, 2006). Principal coordinate analysis (PCoA) based on Bray-Curtis distance was performed using the "vegan" package to show the differences in the prokaryotic community between sites. The relative abundance of community compositions at phylum and genus level were represented by a stack histogram and heatmap, respectively. Linear discriminant analysis effect size was performed among sites to obtain biomarkers with statistical differences and the extent of their effects (Chang et al., 2022). The unique and shared ASVs between sites were calculated and were visualized using a petal chart.

Based on the evolutionary distance of the phylogenetic tree, a null model was

https://doi.org/10.5194/egusphere-2025-1372
Preprint. Discussion started: 8 April 2025

applied to calculate the mean-nearest-taxon distance, which was transformed into the nearest-taxon index (NTI) to reflect the closest interspecific affinities. To obtain the β-nearest-taxon index (βNTI) and describe the spatial and temporal succession of community phylogenetic composition, the β-mean-nearest-taxon distance (βMNTD) was calculated using the comdistnt function in R. The results were divided according to the following conditions: when $|\beta NTI|>2$, the community is in a state of high turnover, which means that the community assembly is controlled by a deterministic process. When $\beta NTI>2$, this indicates heterogenous selection, while $\beta NTI<-2$ indicates that the turnover in community composition is very low, which is interpreted as homogenous selection. When $|\beta NTI|<2$, the community is in a low turnover state, which means a stochastic process is occurring. In this premise, when RCbray>0.95, this means that the Raup-Crick (RC) distance between species is relatively large, which is defined as the dispersal limitation. When RCbray<−0.95, this indicates that the RC distance between species is relatively small and tends to be homogenous, which indicates homogenous dispersal is occurring. Additionally, when $|\beta NTI|<2$ and $|RCbray|<0.95$ are met at the same time, indicating low turnover and a small RC distance, the process is considered to be undominated (e.g. weak selection, weak dispersal, diversification, and drift are occurring).

Spearman's correlation coefficient was calculated and a Mantel test ("linkET" package) was conducted to analyze the correlation between the composition of the microbial community and environment parameters (Legendre and Fortin, 2010).

https://doi.org/10.5194/egusphere-2025-1372
Preprint. Discussion started: 8 April 2025

Random Forest prediction was carried out in the "rfPermute" package (Han and Trimi, 2024) to evaluate the influence of environmental factors such as concentrations of CH_4, SO_4^{2-}, Cl^-, Ca^{2+}, Mg^{2+}, Ba^{2+}, K^+, Fe^{3+}, Cu^{2+}, and Mn^{2+} on microbial distribution at the four stations (ROV1–ROV4).

The bacterial and archaeal communities at each site were used to construct the microbial co-occurrence networks for each site. The ASVs with relative abundance >0.005 were extracted using the "psych" and "igraph" packages. The correlations between individual ASVs were calculated using Spearman's correlation coefficients and the "Benjimini–Hockberg" method was applied to correct the P values of the correlation coefficients. The obtained networks were visualized in Gephi software, and the basic topological properties of the networks were derived, including average degree, average clustering coefficient, average path length and modularity. Average degree indicates the average number of connections between nodes. The clustering coefficient of a node refers to the ratio of the number of connected edges between its neighbors to the maximum number of possible connected edges between these neighbors. Average clustering coefficient is the average of the clustering coefficients of all nodes in the network. Average path length represents the average of the distance between any two nodes. Modularity represents the number and structure of modules composed of nodes in a network.

The visualization of the above analysis was completed in R and Origin software (vers. 2024). The environmental factors, α-diversity boxplots, heatmaps, phylum

https://doi.org/10.5194/egusphere-2025-1372
Preprint. Discussion started: 8 April 2025

community composition and community assembly stacking bar charts, biomarker bar charts, NTI, βNTI scatter plots, and network topology bar charts were all drawn using Origin software. The results of PCoA, a Mantel test, and Random Forest were all visualized using the "ggplot2" package of R software, and a petal diagram was drawn using the "plotrix" package.

https://doi.org/10.5194/egusphere-2025-1372
Preprint. Discussion started: 8 April 2025

3. Results and discussion

3.1 Horizontal geochemical heterogeneity of sediments

The environmental factors of sediments at different Haima cold seeps are shown in the Fig. 1 and Table S1. The changes of geochemical properties were significant along the horizontal profile of the sediments. Higher CH_4, TIC, and Ba^{2+} concentrations were observed at ROV1 sediments than in sediments from the other three sites. In contrast, the ROV1 sediment showed lower TOC, SO_4^{2-}, and Ca^{2+} concentrations. The concentrations of K^+, Mg^{2+}, Fe^{3+}, Cu^{2+}, and Mn^{2+} were not significantly different between sites, and the concentrations of Fe^{3+}, Cu^{2+}, and Mn^{2+} were extremely low.

Significant differences in geochemical properties were found between the methane seep area (ROV1) and the macrobiotic areas (ROV2, ROV3, and ROV4), which were attributed to the different biogeochemical processes. The abundance of methane drove the microbial-mediated anaerobic oxidation of methane (AOM) in ROV1 sediments and coupled sulfate reduction to generate large amounts of HCO_3^-. As a result, relatively higher CH_4 and TIC concentrations and a lower sulfate concentration were observed in ROV1 sediments. The bicarbonate produced by the AOM increased the alkalinity of the surrounding porewater and methane combined with Ca^{2+} to form authigenic carbonates (Akam et al., 2023; Gong et al., 2023). In short, significant horizontal differences were observed in environmental parameters at different locations of the sediments of Haima cold seeps.

3.2 Differences in prokaryotic community diversity of horizontal sediments

https://doi.org/10.5194/egusphere-2025-1372
Preprint. Discussion started: 8 April 2025

A total of 4,016,684 bacterial and 3,288,215 archaeal high-quality sequences were obtained after merging and filtering the raw data of 16S rRNA genes of bacteria and archaea from 28 sediment samples. The bacterial and archaeal reads were clustered to generate 54,081 and 20,180 ASVs, respectively. The average value of Goods coverage (Fig. S1) in each site was greater than 0.99, indicating that the sequencing depth of all samples was sufficient to cover all species in the samples. The α-diversities of bacterial and archaeal communities at sites are shown in Figs. 2a, 3a, and Table S2. The Chao1, Observed ASVs, Phylogenetic diversity, and Shannon indices revealed the horizontal differences of microbial α-diversity in different sediments. The bacterial α-diversity peaked at the ROV2 site and the lowest value at ROV1. The α-diversity of archaeal communities was the lowest at ROV1, and was significantly different from the other three sites.

The community variability between samples can be visualized using PCoA. The first two principal coordinates explained 40.23% and 54.99% of the variance in the bacterial and archaeal communities, respectively (Figs. 2b and 3b, respectively). The bacterial and archaeal communities from the same site clustered together and varied in different site sediments. The bacterial community of ROV1, ROV2, ROV3, and ROV4 were mainly concentrated in the third, fourth, first, and first quadrants, respectively. The PCoA of the archaeal community showed a similar trend. To further confirm similarity and discrepancy among samples, a petal chart based on the ASV composition was created; the results showed that samples grouped by site had more shared ASVs

https://doi.org/10.5194/egusphere-2025-1372
Preprint. Discussion started: 8 April 2025

than those grouped by depth (Fig. S2) in both bacterial and archaeal communities. The compositions of the bacterial (Fig. 2c) and archaeal (Fig. 3c) communities at each site were analyzed at the phylum level. In the bacterial community, Desulfobacterota (13.8%−29.7%) were more frequent in the ROV1 site than in other sites. Chloroflexi (11.8%−45.9%) was the dominant phyla of ROV2. Meanwhile, ROV3 had relatively high concentrations of Chloroflexi (10.4%−39.2%) and Proteobacteria (12.5%−43.9%). Proteobacteria (10.9%−29.3%), Chloroflexi (8.1%−22.9%) and Desulfobacterota (13.3%−20.6%) were the dominant phyla of site ROV4. In the archaeal community, Halobacterota (77%−91.5%) was the main group at the ROV1 site. Asgardarchaeota (12.9%−51.7%), Crenarchaeota (4.0%−44.5%), and Halobacterota (5.5%−37.7%) were the principal phyla of ROV2. Halobacterota (8.5%−62.3% and 24.1%−67.9%), Thermoplasmatota (1.7%−14.7% and 11.1%−24.2%), and Asgardarchaeota (6.4%−35.7% and 3.7%−11.1%) were the dominant taxa of both ROV3 and ROV4, but ROV3 had more Firmicutes (0.7%−15.2%) and Proteobacteria (3.3%−28.2%) than ROV4. In addition, community composition at the genus level was also investigated (Fig. S3). In the bacterial community, *JS1* was dominant in ROV1, ROV3, and ROV4. In addition, *Anaerolineaceae* and *Dehalococcoidia* dominated in ROV2. *Anaerolineaceae* was also relatively frequent in ROV3. In the archaeal community, ROV1 was dominated by *ANME-1b* and *ANME-2c*. *Lokiarchaeia* and *Bathyarchaeia* were dominant in ROV2. In addition, *ANME-1a* mainly inhabited ROV3 and ROV4. The linear discriminant analysis effect size method was used to compare ASVs between

https://doi.org/10.5194/egusphere-2025-1372
Preprint. Discussion started: 8 April 2025

sites and identify biomarkers in bacterial (Fig. 2d) and archaeal (Fig. 3d) communities. The dominant classes of bacterial communities in ROV1 included Dissulfuribacteria, Methanosarcinia and Gammaproteobacteria. Dehalococcoidia was the main class found at site ROV2. Both ROV3 and ROV4 had habitat of taxa in the class Gammaproteobacteria. In addition, abundant taxa in the class Bacilli were also found in ROV3. In the archaeal community, ANME-1 and Methanosarcinia had been identified as the biomarkers for ROV1 and ROV4. Also, ANME-1 was a major member of the Halobacterota. Meanwhile, *ANME-1b* and *ANME-2c* existed in ROV1, while *ANME-1a* appeared in ROV4. The ROV2 site was the representative territory of Lokiarchaeia and Thermoplasmata. Rich Gammaproteobacteria and Bacilli appeared frequently in ROV3.

Differences in biogeological parameters play crucial roles on the formation of distinct biological communities (Li et al., 2021; Zhai et al., 2022; Zhang et al., 2015). Both environmental conditions and physical distance are important factors affecting microbial community structure (Martiny et al., 2006). The flux and duration of seepage are the driving factors of faunal colonization (Seabrook et al., 2018). The microbial-mediated AOM serves as the principal method of methane consumption in sediments, which is mainly achieved by anaerobic methanotrophic archaea (ANME) and SRB (Zhai et al., 2022). For example, site ROV1 was in the early stage of a cold seep and sediments here were dominated by methane oxidation and sulfate reduction. In addition, ANME and SRB were the dominant microorganisms in ROV1, where the community

https://doi.org/10.5194/egusphere-2025-1372
Preprint. Discussion started: 8 April 2025

diversity was relatively simple as shown by the relatively low α-diversity at this site. Meanwhile, the other three sites were in the middle and late stages of cold seep formation where diverse microorganisms were enriched and provided biomass energy for the overlying fauna. Consequently, the relative higher α-diversities were observed at the other three sites. The sample aggregation and site distance displayed by PCoA further confirmed the discrepancies between microbial communities of different cold seep habitats.

Gammaproteobacteria have been identified as a dominant bacterial taxon in deep sea sediments and have the potential to degrade oil contaminants in marine environments (Aoki et al., 2014; Cui et al., 2019). Desulfobacteraceae, a cluster of Desulfobacterota, are believed to cooperate with ANME to complete the sulfate-driven anaerobic oxidation of methane (Cui et al., 2019). The relatively high methane content and biomarkers of ROV1 suggested that ANME-1b and ANME-2c might collaborate with Desulfobacterota for AOM. Chloroflexi usually occurs in anaerobic or organic-rich sediments, and in particular, the class Dehalococcoidia has been shown to oxidize aromatic compounds (Pöritz et al., 2015; Wasmund et al., 2014; Zanaroli et al., 2012). Lokiarchaeia is a branch of the phylum Asgardarchaeota and are heterotrophic archaea involved in anaerobic fermentation; Lokiarchaeia have been considered to be one of the important members of the carbon cycle in sediment ecosystems (Busi et al., 2021). Lokiarchaeia (Spang et al., 2015) were first discovered in sediments near the Loki's Castle active vent site. This group is thought to be involved in the oxidation of methane

https://doi.org/10.5194/egusphere-2025-1372
Preprint. Discussion started: 8 April 2025

and in sulfate reduction metabolism (Cai et al., 2021). Thermoplasmatota are host-associated or free-living methanogens (Bendia et al., 2022).

In summary, Desulfobacterota and Halobacterota existed in ROV1 areas where relatively strong sulfate reduction and anaerobic oxidation of methane occurred. Chloroflexi and Asgardarchaeota were relatively abundant in sediments at middle and lower depths, suggesting that the microbial reaction intensity of site ROV2 was greater at these depths. Accordingly, similarity of environmental conditions of ROV3 and ROV4 resulted in similar microbial community composition, with mainly Proteobacteria and Halobacterota present. In general, the heterogeneous composition of prokaryotes was caused by dissimilar environmental conditions. Differences in seepage flow led to diversity of environmental parameters, further promoting the composition of different microorganisms.

3.3 Horizontal environmental heterogeneity affects prokaryotic community diversity

To detect the influence of environmental variables on prokaryotic communities, a Mantel test (Fig. 4a) and Random Forest model analysis (Fig. 4b) were performed which depended on prokaryotic communities and environmental parameters. Mantel test results showed that environmental factors that had significant effects on the diversity of bacterial and archaeal communities were CH_4, TIC, SO_4^{2-}, Ca^{2+}, Ba^{2+}, and Mg^{2+} ($p<0.01$, $r>=0.4$). Random Forest results showed that the concentrations of CH_4, Ba^{2+}, Ca^{2+}, SO_4^{2-}, and TIC had significant effects on the microbial community structure at different sites ($p<0.01$); the Mean Decrease Accuracy value of CH_4 was the highest

https://doi.org/10.5194/egusphere-2025-1372
Preprint. Discussion started: 8 April 2025

(25.29%), indicating that methane had the most significant effect on the structure of the microbial community.

The aggregation of microorganisms in cold seep sediment had obvious biogeographical distribution characteristics, which were related to in-situ geochemical conditions, such as the concentrations of methane and sulfate (Heijs et al., 2007; Jiang et al., 2022). The emission of seepage fluids from cold seeps shaped microbial communities in these environments, especially anaerobic methanotroph communities (Vigneron et al., 2019). In hydrate-bearing ecosystems, it can be reasonably hypothesized that CH_4 can affect microorganisms; several studies have shown that methane leakage is correlated with the structure of the surrounding microbial community (Li et al., 2021; Zhang et al., 2012). Methanotrophic microorganisms are often coupled with sulfate-reducing bacteria, which are thought to be the main force involved in the production and consumption of sulfate (Xu et al., 2020). In addition, HCO_3^- combines with Ca^{2+} to form carbonate rocks, which consume calcium ions. The concentration of SO_4^{2-} and Ca^{2+} in the ROV1 site decreased, suggesting an increase in the intensity of AOM at this site (Chen et al., 2023). Combined with the differences of environmental factors and microbial communities at each site, it was speculated that environmental parameters, especially concentrations of CH_4, TIC, SO_4^{2-}, and Ca^{2+}, were correlated with microbial community structure. These parameters are important parts of the chemosynthesis reactions driven by microorganisms in cold seepage environments.

https://doi.org/10.5194/egusphere-2025-1372
Preprint. Discussion started: 8 April 2025

The seepage activity in the Haima cold seeps region changes with time and space (Xu et al., 2020). Therefore, the intensity of external leakage of different sites will vary, so that the energy and nutrition will fundamentally support different prokaryote taxa and functional community structure (Chen et al., 2023). In that study, the changes of AOM related parameters and the role of microbial functional groups in biogeology suggest a link between environmental parameters and microbial community structure.

3.4 Horizontal environmental heterogeneity drives different community assembly processes of prokaryotic communities

To explore the assembly process of prokaryotic communities at different sites, the assembly mechanism of bacterial and archaeal communities was predicted on a horizontal scale based on a null model (Fig. 5). The NTI and Shannon diversity indices were positively correlated, indicating that the community phylogeny varied with community diversity (Fig. 5a and 5b). Bacterial βNTI was positively correlated with differences in environmental parameters of CH_4, TIC, SO_4^{2-}, and Ca^{2+} ($p<0.001$) (Fig. 5e), while archaeal βNTI was negatively correlated with differences in environmental parameters ($p<0.001$) (Fig. 5f), indicating that these parameters were important factors affecting community assembly. The bacterial community assembly was mainly driven by stochastic processes (Fig. 5c), while deterministic and stochastic processes contributed to the assembly process of the archaeal community (Fig. 5d). In the assembly process of the bacterial community, the community of the ROV1 site was mainly influenced by homogenizing dispersal (33.3%) along with undominated (23.8%)

https://doi.org/10.5194/egusphere-2025-1372
Preprint. Discussion started: 8 April 2025

and homogeneous selection (33.3%), while dispersal limitation (28.6−52.4%) and homogeneous selection (28.6−61.9%) played more important roles at other sites. In the archaeal community, deterministic processes (homogenous and heterogeneous selection processes) dominated the communities at all sites. Especially in communities of ROV1, homogenous selection (85.7%) almost completely dominated the archaeal community. The archaeal communities at ROV2 and ROV3 were jointly affected by homogenous selection (23.8−42.8%), heterogenous selection (33.3−38.1%) and undominant selection (23.8−33.3%). In the community of ROV4, homogenous selection (57.1%) and undominant process (38.1%) were the main driving forces.

In general, deterministic processes control community composition and turnover, but stochastic processes also play an important role (Stegen et al., 2012). The bacterial communities in that study were strongly influenced by stochastic processes, and the assembly of archaeal communities was affected by stochastic and deterministic processes. In conclusion, the diverse assembly processes of bacterial and archaeal communities were the result of environmental heterogeneity at different sites.

In the present study, environmental parameters differed among sites and the environmental difference affected the assembly process of the microbiome. The interaction of methane-related substances was an important factor that promotes microbial aggregation. Stochastic processes become more vital to community assembly in highly productive environments (Chase, 2010). Consistently, in systems with high levels of chemosynthesis such as those with methane seepage, the community assembly

https://doi.org/10.5194/egusphere-2025-1372
Preprint. Discussion started: 8 April 2025

of the prokaryotes in the present study was primarily influenced by stochastic processes. Environmental heterogeneity affected the aggregation of microorganisms, which further led to the alteration in assembly processes at different locations. The assembly of biomes is generally affected by stochastic and deterministic factors, and they may synergistically affect the diversity of biomes (Soininen and Graco-Roza, 2024). In this study, stochastic and deterministic processes showed different response balances in prokaryotic communities at different sites. The bacterial community of the ROV1 site was more affected by stochastic processes (homogenizing dispersal and undominated) than at the three other sites and the biodiversity was relatively low. It might be a result of the high content of nutrients such as methane in ROV1, which was conducive to supporting the growth of specific microorganisms. The high dispersal rate in the region may lead to the homogenization of the community and the formation of similar community composition in different areas (Zhou and Ning, 2017). The assembly of the archaeal community at the ROV1 site was mainly the result of homogenous selection. In highly productive environments, the colonization of dominant species tends to result in the establishment of populations with a very stable equilibrium (Chase, 2010). Methane-oxidizing archaea, as the dominant group of competitive species, settled in large numbers at the ROV1 site, the components of which were relatively concentrated but with low biodiversity. Microorganisms can respond to the competitive pressure caused by the environment (Dai et al., 2017). Homogeneous environmental conditions are likely to favor similar species composition and community structure at various sites

https://doi.org/10.5194/egusphere-2025-1372
Preprint. Discussion started: 8 April 2025

(Wu et al., 2021). In the samples of sites ROV2, ROV3, and ROV4, the relatively low methane content was similar at different depths, resulting in similar homogenous selection at these sites. Accordingly, the environmental heterogeneity between sites also leads to the control of prokaryotic community assembly by different degrees of homogenous selection.

In conclusion, environmental parameters as significant factors affecting the colonization activity of microbes, play a role in shaping community structure. Horizontal discrepancy in ambient conditions result in a balance between the differences in assembly processes, such as stochastic and deterministic processes. The heterogeneity of the horizontal nutrient distribution in four sites in the Haima cold seeps area drove the diversity of prokaryotic community assembly.

3.5 Coexistence patterns of different species in prokaryotic communities vary along the horizontal sediment dimension

In the present study, the co-occurrence networks and topological properties are shown to assess microbial associations (Fig. 6). In the bacterial community co-occurrence networks (Fig. 6a), more connections were shown between the microorganisms of the ROV1 site than at other sites. In the archaeal community (Fig. 6b), the microbial network of ROV1 had fewer nodes and connections when compared with other sites. The majority of species in the bacterial networks belonged to Chloroflexi, Desulfobacterota, and Proteobacteria. In the archaeal networks, species mainly belonged to Thermoplasmatota, Halobacterota, Asgardarchaeota, and

https://doi.org/10.5194/egusphere-2025-1372
Preprint. Discussion started: 8 April 2025

Crenarchaeota. The topological properties of the prokaryotic networks were different among the sites (Fig. 6c and 6d). The bacterial network of ROV1 showed more node connections, while the archaeal network did the opposite, indicating that bacterial species communicated more frequently with each other than archaeal species. For example, the average degree of bacterial communication at ROV1 was the highest, while the average degree of archaeal communication was the lowest. The network of ROV3 exhibited more intense clustering and modularity, indicating the close association and structural stability of the microbial communities at this site.

As a high methane seepage area, the microbial network of the ROV1 site was different from other sites. Bacterial co-occurrence networks in ROV1 showed higher species connectivity. The high connectivity and short average path length indicates that external disturbances could transfer swiftly between nodes in the network, which enhances the overall efficiency of the system (Wu et al., 2024). However, low modularity also reflected the instability of the bacterial community at this site. Modularity can reflect interactions such as competition, cooperation, and niche differentiation among microorganisms, which increase the complexity of ecological networks (Zhang et al., 2020). In contrast, the species connectivity of the archaeal community at ROV1 was significantly lower than that at other sites, and the degree of modularity of the network was higher, suggesting that the archaeal community at this site was relatively stable. This fact may be a result of the supply of cold fluids and specific microbial responses to environmental selection resulting in distinct system

https://doi.org/10.5194/egusphere-2025-1372
Preprint. Discussion started: 8 April 2025

divisions. Very abundant taxa are more frequently located in the center of the network (Zhang et al., 2020). The major species of ROV2 were located in the center of the network and the connectivity was high, indicating the major species uniformity found at the ROV2 site and their irreplaceable roles in the community. The short average path length and medium modularity suggested that although microbial co-occurrence and interaction were more frequent in oligotrophic environments, the stability of the network was not adequate to maintain the network over time.

The ROV1 site exhibited unique microbial co-occurrence with other sites. The important role of microbes in the chemosynthesis system meant the archaea at this site exhibited more unique patterns in terms of species diversity and community interactions compared to other sites. The differences in the other site environments were not prominent, but slight differences were still observed in the co-occurrence process. The environment creates ecological niches that allow for the interaction and reproduction of dominant species, playing a crucial role in structuring microbial communities (Freilich et al., 2018). The content of methane and its related series of reactions drove the surrounding microbial activities, driving microbial adaptation to the environment and selective colonization. In this process, microbial interactions and environmental forces had great significance for the development of biological communities and the formation of ecological networks at this site (Kraft et al., 2015). Environmental differences initially drove the aggregation of prokaryotes, selected for suitable species in the ecosystem, and facilitated the further development of different coexisting networks

https://doi.org/10.5194/egusphere-2025-1372
Preprint. Discussion started: 8 April 2025

through evolutionary processes such as competition. Eventually, the influence of the environment on the development of the biological community reflected the adaptation and evolutionary succession of prokaryotes to different habitats in the extreme environment of cold seeps.

https://doi.org/10.5194/egusphere-2025-1372
Preprint. Discussion started: 8 April 2025

4. Conclusions

Through a comprehensive investigation of sediment microorganisms from different sampling sites in the Haima cold seeps, differences were found in prokaryotic community assembly and species coexistence patterns among the four sampling sites in the present study. Significant differences in the abundance and community structure of microorganisms were found in regions with different methane content. The results of β-NTI showed that the assembly process of prokaryotic communities at each site was mainly controlled by stochastic processes. Specifically, the archaeal communities in areas with high methane content might be driven by the same energy source, and the assembly process also exhibited a significant degree of determinacy. Horizontal environmental heterogeneity affected the diversity and structure of prokaryotic communities, driving the assembly process of bacteria and archaea. Different co-occurrence networks further showed the diversity of species coexistence patterns in different environments. In conclusion, the present study explored environmental heterogeneity observed at different locations in the cold seep from a microbiological perspective, deepening our understanding of how environmental heterogeneity plays an important role in the assembly of prokaryotic communities and species coexistence.

Data availability

All raw sequences in this study have been deposited at the NCBI Sequence Read Archive under the accession number PRJNA1230284.

https://doi.org/10.5194/egusphere-2025-1372
Preprint. Discussion started: 8 April 2025

Author contribution:

Qixuan Wu: Investigation, Formal Analysis, Writing - Original Draf

Jingchun Feng: Conceptualization, Funding Acquisition, Resources, Supervision, Writing - Review & Editing

Yongji Huang: Visualization

Song Zhong: Visualization

Cun Li: Visualization

Si Zhang: Resources, Supervision

ACKNOWLEDGEMENT

This work was financially supported by the National Natural Science Foundation of China (42325603, 42227803, 42449303, and 42494884), the National Key Research and Development Program of China (2021YFF0502300), the Guangdong Natural Resources Foundation (GDNRC[2023]30), the PI project of Southern Marine Science and Engineering Guangdong Laboratory (Guangzhou) (GML20190609, GML2022009, and GML20230921) are gratefully acknowledged.

https://doi.org/10.5194/egusphere-2025-1372
Preprint. Discussion started: 8 April 2025

References:

Akam SA, Swanner ED, Yao HM, Hong WL, Peckmann J. Methane-derived authigenic carbonates-A case for a globally relevant marine carbonate factory. Earth-Science Reviews 2023; 243.

Aoki M, Ehara M, Saito Y, Yoshioka H, Miyazaki M, Saito Y, et al. A Long-Term Cultivation of an Anaerobic Methane-Oxidizing Microbial Community from Deep-Sea Methane-Seep Sediment Using a Continuous-Flow Bioreactor. Plos One 2014; 9.

Bendia AG, Nakamura FM, Butarelli ACD, Kmit MCP, Ramos RB, Signori CN, et al. First description of archaeal communities in carbonate-rich seafloor and subseafloor sediments from the Southwestern Atlantic slope. Ocean and Coastal Research 2022; 70.

Busi SB, de Nies L, Habier J, Wampach L, Fritz JV, Heintz-Buschart A, et al. Recoding of stop codons expands the metabolic potential of two novel Asgardarchaeota lineages. Isme Communications 2021; 1.

Cai MW, Richter-Heitmann T, Yin XR, Huang WC, Yang YC, Zhang CJ, et al. Ecological features and global distribution of Asgard archaea. Science of the Total Environment 2021; 758.

Chang F, He SS, Dang CY. Assisted Selection of Biomarkers by Linear Discriminant Analysis Effect Size (LEfSe) in Microbiome Data. Jove-Journal of Visualized Experiments 2022.

Chase JM. Stochastic Community Assembly Causes Higher Biodiversity in More Productive Environments. Science 2010; 328: 1388-1391.

Chase JM, Myers JA. Disentangling the importance of ecological niches from stochastic processes across scales. Philosophical Transactions of the Royal Society B-Biological Sciences 2011; 366: 2351-2363.

Chen Y, Dai TJ, Li N, Li QQ, Lyu Y, Di PF, et al. Environmental heterogeneity shapes the C and S cycling-associated microbial community in Haima's cold seeps. Frontiers in Microbiology 2023; 14.

Cui HP, Su X, Chen F, Holland M, Yang SX, Liang JQ, et al. Microbial diversity of two cold seep systems in gas hydrate-bearing sediments in the South China Sea. Marine Environmental Research 2019; 144: 230-239.

Dai WF, Zhang JJ, Tu QC, Deng Y, Qiu QF, Xiong JB. Bacterioplankton assembly and interspecies interaction indicating increasing coastal eutrophication. Chemosphere 2017; 177: 317-325.

Dong XY, Peng YY, Wang MH, Woods L, Wu WX, Wang Y, et al. Evolutionary ecology of microbial populations inhabiting deep sea sediments associated with cold seeps. Nature Communications 2023; 14.

Duperron S, Guezi H, Gaudron SM, Ristova PP, Wenzhöfer F, Boetius A. Relative abundances of methane- and sulphur-oxidising symbionts in the gills of a cold seep mussel and link to their potential energy sources. Geobiology 2011; 9: 481-491.

https://doi.org/10.5194/egusphere-2025-1372
Preprint. Discussion started: 8 April 2025

585 Duperron S, Halary S, Lorion J, Sibuet M, Gaill F. Unexpected co-occurrence of six
586 bacterial symbionts in the gills of the cold seep mussel *Idas* sp (Bivalvia:
587 Mytilidae). Environmental Microbiology 2008; 10: 433-445.
588 Duperron S, Sibuet M, MacGregor BJ, Kuypers MMM, Fisher CR, Dubilier N.
589 Diversity, relative abundance and metabolic potential of bacterial endosymbionts
590 in three *Bathymodiolus* mussel species from cold seeps in the Gulf of Mexico.
591 Environmental Microbiology 2007; 9: 1423-1438.
592 Feng D, Qiu JW, Hu Y, Peckmann J, Guan HX, Tong HP, et al. Cold seep systems in
593 the South China Sea: An overview. Journal of Asian Earth Sciences 2018; 168: 3-
594 16.
595 Feng JC, Li CR, Tang L, Wu XN, Wang Y, Yang ZF, et al. Tracing the Century-Long
596 Evolution of Microplastics Deposition in a Cold Seep. Advanced Science 2023a;
597 10.
598 Feng JC, Yang ZF, Zhou WL, Feng XW, Wei FW, Li B, et al. Interactions of
599 Microplastics and Methane Seepage in the Deep-Sea Environment. Engineering
600 2023b; 29: 159-167.
601 Freilich MA, Wieters E, Broitman BR, Marquet PA, Navarrete SA. Species co-
602 occurrence networks: Can they reveal trophic and non-trophic interactions in
603 ecological communities? Ecology 2018; 99: 690-699.
604 Gong SG, Luo M, Griffith EM, Peckmann J, Liang QY, Feng D. Calcium isotopic
605 fractionation during aragonite and high-Mg calcite precipitation at methane seeps.
606 Earth and Planetary Science Letters 2023; 622.
607 Gravel D, Guichard F, Hochberg ME. Species coexistence in a variable world. Ecology
608 Letters 2011; 14: 828-839.
609 Han H, Trimi S. Analysis of cloud computing-based education platforms using
610 unsupervised random forest. Education and Information Technologies 2024.
611 Heijs SK, Haese RR, van der Wielen P, Forney LJ, van Elsas JD. Use of 16S rRNA
612 gene based clone libraries to assess microbial communities potentially involved
613 in anaerobic methane oxidation in a Mediterranean cold seep. Microbial Ecology
614 2007; 53: 384-398.
615 Hu Y, Luo M, Liang QY, Chen LY, Feng D, Yang SX, et al. Pore fluid compositions and
616 inferred fluid flow patterns at the Haima cold seeps of the South China Sea.
617 Marine and Petroleum Geology 2019; 103: 29-40.
618 Jiang QY, Jing HM, Liu H, Du MR. Biogeographic distributions of microbial
619 communities associated with anaerobic methane oxidation in the surface
620 sediments of deep-sea cold seeps in the South China Sea. Frontiers in
621 Microbiology 2022; 13.
622 Kraft NJB, Adler PB, Godoy O, James EC, Fuller S, Levine JM. Community assembly,
623 coexistence and the environmental filtering metaphor. Functional Ecology 2015;
624 29: 592-599.
625 Lee OO, Wang Y, Tian RM, Zhang WP, Shek CS, Bougouffa S, et al. *In situ*
626 environment rather than substrate type dictates microbial community structure of

https://doi.org/10.5194/egusphere-2025-1372
Preprint. Discussion started: 8 April 2025

biofilms in a cold seep system. Scientific Reports 2014; 4.
Legendre P, Fortin MJ. Comparison of the Mantel test and alternative approaches for detecting complex multivariate relationships in the spatial analysis of genetic data. Molecular Ecology Resources 2010; 10: 831-844.
Li XP, Dai ZH, Di PF, Feng JX, Tao J, Chen DF, et al. Distinct Bottom-Water Bacterial Communities at Methane Seeps With Various Seepage Intensities in Haima, South China Sea. Frontiers in Marine Science 2021; 08.
Liang QY, Hu Y, Feng D, Peckmann J, Chen LY, Yang SX, et al. Authigenic carbonates from newly discovered active cold seeps on the northwestern slope of the South China Sea: Constraints on fluid sources, formation environments, and seepage dynamics. Deep-Sea Research Part I-Oceanographic Research Papers 2017; 124: 31-41.
Lin ZY, Sun XM, Chen KY, Strauss H, Klemd R, Smrzka D, et al. Effects of sulfate reduction processes on the trace element geochemistry of sedimentary pyrite in modern seep environments. Geochimica Et Cosmochimica Acta 2022; 333: 75-94.
Lyu Y, Zhang J, Chen Y, Li QQ, Ke ZX, Zhang S, et al. Distinct diversity patterns and assembly mechanisms of prokaryotic microbial sub-community in the water column of deep-sea cold seeps. Journal of Environmental Management 2023; 348.
Martiny JBH, Bohannan BJM, Brown JH, Colwell RK, Fuhrman JA, Green JL, et al. Microbial biogeography:: putting microorganisms on the map. Nature Reviews Microbiology 2006; 4: 102-112.
Meier U. A note on the power of Fisher's least significant difference procedure. Pharmaceutical Statistics 2006; 5: 253-263.
Ning DL, Yuan MT, Wu LW, Zhang Y, Guo X, Zhou XS, et al. A quantitative framework reveals ecological drivers of grassland microbial community assembly in response to warming. Nature Communications 2020; 11.
Niu MY, Deng LH, Su L, Ruff SE, Yang N, Luo M, et al. Methane supply drives prokaryotic community assembly and networks at cold seeps of the South China Sea. Molecular Ecology 2023; 32: 660-679.
Pöritz M, Schiffmann CL, Hause G, Heinemann U, Seifert J, Jehmlich N, et al. *Dehalococcoides mccartyi* Strain DCMB5 Respires a Broad Spectrum of Chlorinated Aromatic Compounds. Applied and Environmental Microbiology 2015; 81: 587-596.
Seabrook S, De Leo FC, Baumberger T, Raineault N, Thurber AR. Heterogeneity of methane seep biomes in the Northeast Pacific. Deep-Sea Research Part Ii-Topical Studies in Oceanography 2018; 150: 195-209.
Soininen J, Graco-Roza C. Homogeneous selection and stochasticity overrule heterogeneous selection across biotic taxa and ecosystems. Oikos 2024.
Spang A, Saw JH, Jorgensen SL, Zaremba-Niedzwiedzka K, Martijn J, Lind AE, et al. Complex archaea that bridge the gap between prokaryotes and eukaryotes. Nature 2015; 521: 173-+.

https://doi.org/10.5194/egusphere-2025-1372
Preprint. Discussion started: 8 April 2025

669 Stegen JC, Lin XJ, Konopka AE, Fredrickson JK. Stochastic and deterministic
670 assembly processes in subsurface microbial communities. Isme Journal 2012; 6:
671 1653-1664.
672 Sun QL, Zhang J, Wang MX, Cao L, Du ZF, Sun YY, et al. High-Throughput
673 Sequencing Reveals a Potentially Novel *Sulfurovum* Species Dominating the
674 Microbial Communities of the Seawater-Sediment Interface of a Deep-Sea Cold
675 Seep in South China Sea. Microorganisms 2020; 8.
676 Takai K, Horikoshi K. Rapid detection and quantification of members of the archaeal
677 community by quantitative PCR using fluorogenic probes. Applied and
678 Environmental Microbiology 2000; 66: 5066-+.
679 Vigneron A, Alsop EB, Cruaud P, Philibert G, King B, Baksmaty L, et al. Contrasting
680 Pathways for Anaerobic Methane Oxidation in Gulf of Mexico Cold Seep
681 Sediments. Msystems 2019; 4.
682 Wasmund K, Schreiber L, Lloyd KG, Petersen DG, Schramm A, Stepanauskas R, et al.
683 Genome sequencing of a single cell of the widely distributed marine subsurface
684 *Dehalococcoidia*, phylum *Chloroflexi*. Isme Journal 2014; 8: 383-397.
685 Wennekes PL, Rosindell J, Etienne RS. The Neutral-Niche Debate: A Philosophical
686 Perspective. Acta Biotheoretica 2012; 60: 257-271.
687 Whitfield J. Ecology: Neutrality versus the niche. Nature 2002; 417: 480-481.
688 Wu H, Gao TH, Hu A, Wang JJ. Network Complexity and Stability of Microbes
689 Enhanced by Microplastic Diversity. Environmental Science & Technology 2024;
690 58: 4334-4345.
691 Wu WX, Xu ZM, Dai MH, Gan JP, Liu HB. Homogeneous selection shapes free-living
692 and particle-associated bacterial communities in subtropical coastal waters.
693 Diversity and Distributions 2021; 27: 1904-1917.
694 Xu HC, Du MR, Li JT, Zhang HB, Chen WL, Wei JG, et al. Spatial distribution of
695 seepages and associated biological communities within Haima cold seep field,
696 South China Sea. Journal of Sea Research 2020; 165.
697 Yu Y, Lee C, Kim J, Hwang S. Group-specific primer and probe sets to detect
698 methanogenic communities using quantitative real-time polymerase chain
699 reaction. Biotechnology and Bioengineering 2005; 89: 670-679.
700 Zanaroli G, Balloi A, Negroni A, Borruso L, Daffonchio D, Fava F. A Chloroflexi
701 bacterium dechlorinates polychlorinated biphenyls in marine sediments under *in*
702 *situ*-like biogeochemical conditions. Journal of Hazardous Materials 2012; 209:
703 449-457.
704 Zhai X, Shi X, Cheng H, Yao P, Zhao B, Chen L, et al. Horizontal and vertical
705 heterogeneity of sediment microbial community in Site F cold seep, the South
706 China Sea. Frontiers in Marine Science 2022; 9.
707 Zhang HJ, Hou FR, Xie WJ, Wang K, Zhou XY, Zhang DM, et al. Interaction and
708 assembly processes of abundant and rare microbial communities during a diatom
709 bloom process. Environmental Microbiology 2020; 22: 1707-1719.
710 Zhang J, Sun Q-l, Zeng Z-g, Chen S, Sun L. Microbial diversity in the deep-sea

https://doi.org/10.5194/egusphere-2025-1372
Preprint. Discussion started: 8 April 2025

711 sediments of Iheya North and Iheya Ridge, Okinawa Trough. Microbiological
712 Research 2015; 177: 43-52.
713 Zhang Y, Su X, Chen F, Wang YY, Jiao L, Dong HL, et al. Microbial diversity in cold
714 seep sediments from the northern South China Sea. Geoscience Frontiers 2012;
715 3: 301-316.
716 Zhong S, Feng JC, Kong J, Huang YJ, Chen X, Zhang S. Differences in Bacterial Co-
717 Occurrence Networks and Ecological Niches at the Surface Sediments and
718 Bottom Seawater in the Haima Cold Seep. Microorganisms 2023; 11.
719 Zhou JZ, Ning DL. Stochastic Community Assembly: Does It Matter in Microbial
720 Ecology? Microbiology and Molecular Biology Reviews 2017; 81.
721

https://doi.org/10.5194/egusphere-2025-1372
Preprint. Discussion started: 8 April 2025

722 **Figures:**

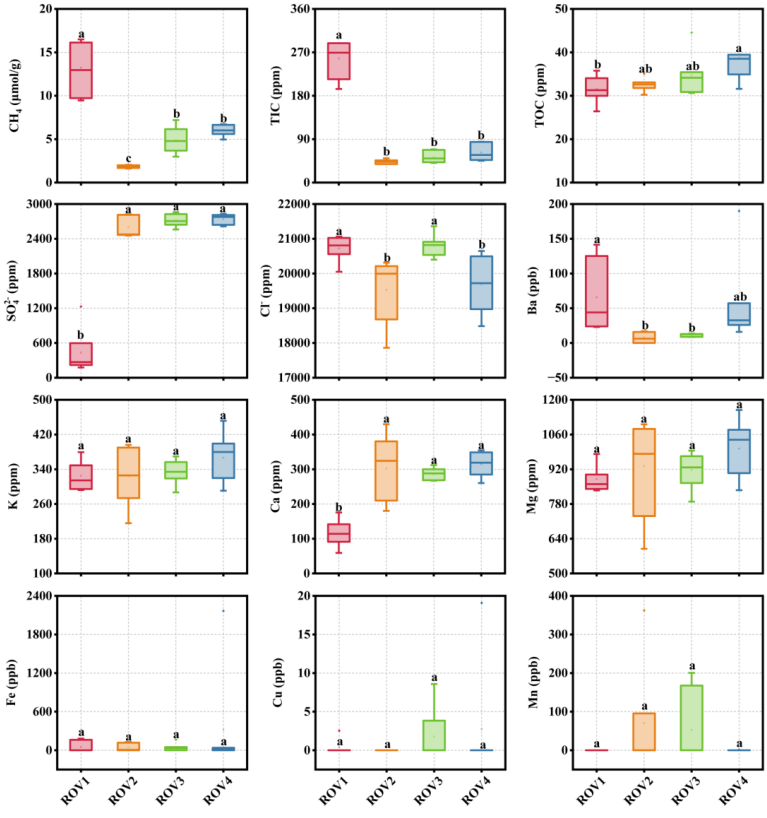

723

724 Fig. 1. Horizontal geochemical properties of sediment samples from four sites of Haima
725 cold seeps in the South China Sea. Letter inconsistencies between the data for the sites
726 ROV1, ROV2, ROV3, and ROV4 indicate significant differences between the sites
727 ($p<0.05$; least significant difference test): concentration of (a) CH_4, (b) total inorganic
728 carbon (TIC), (c) total organic carbon (TOC), and concentrations of (d) SO_4^{2-}, (e) Cl^-,
729 (f) Ba^{2+}, (g) K^+, (h) Ca^{2+}, (i) Mg^{2+}, (j) Fe^{3+}, (k) Cu^{2+}, and (l) Mn^{2+}.

730

731

https://doi.org/10.5194/egusphere-2025-1372
Preprint. Discussion started: 8 April 2025

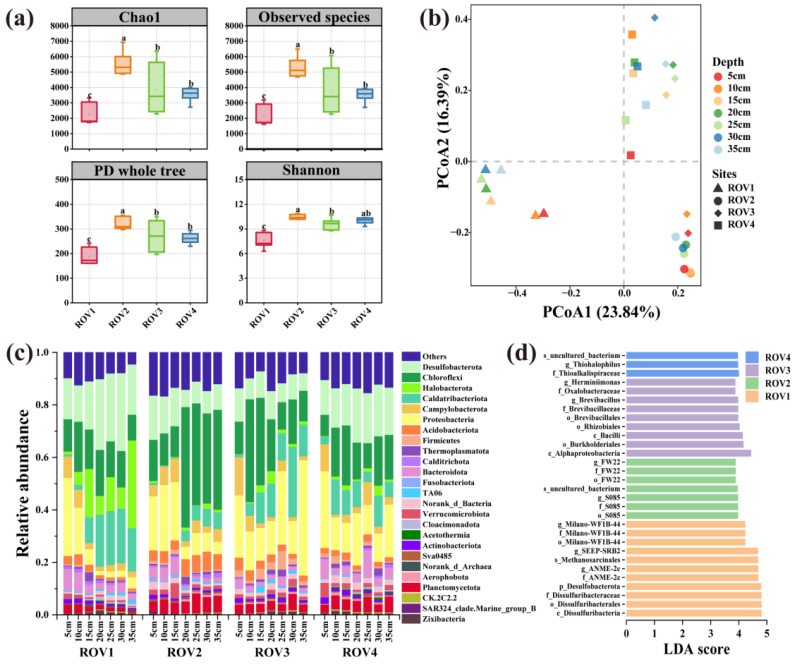

732

733 Fig. 2. Horizontal community composition of bacteria for the sites ROV1, ROV2,
734 ROV3, and ROV4: (a) horizontal α-diversity; letter inconsistencies between the data
735 indicate significant differences between the sites ($p<0.05$; least significant difference
736 test); (b) principal coordinate analysis showing differences in community composition
737 between sites; (c) relative abundance of microbial communities at the phylum level at
738 sites; (d) linear discriminant analysis effect size showing biomarker microorganisms in
739 sediment at different sites. Note: LDA, linear discriminant analysis; PCo1 and PCo2,
740 principal coordinates 1 and 2, respectively.

741

https://doi.org/10.5194/egusphere-2025-1372
Preprint. Discussion started: 8 April 2025

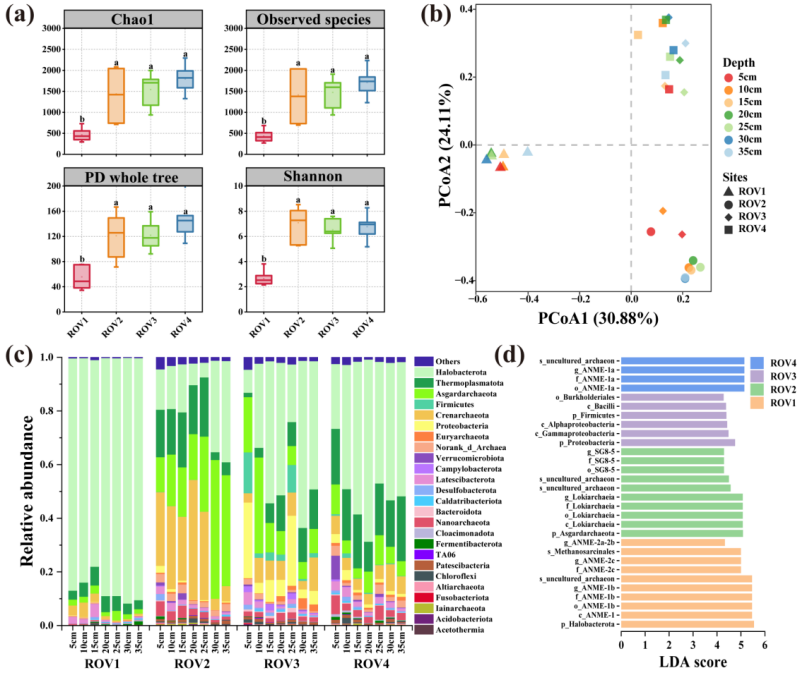

742

743 Fig. 3. Horizontal community composition of Archaea for the sites ROV1, ROV2,
744 ROV3, and ROV4: (a) horizontal α-diversity; letter inconsistencies between the data
745 indicate significant differences between the sites ($p<0.05$; least significant difference
746 test); (b) principal coordinate analysis showing differences in community composition
747 between sites; (c) relative abundance of microbial communities at the phylum level at
748 sites; (d) linear discriminant analysis effect size showing biomarker microorganisms in
749 sediment at different sites. Note: LDA, linear discriminant analysis; PCo1 and PCo2,
750 principal coordinates 1 and 2, respectively.

751

https://doi.org/10.5194/egusphere-2025-1372
Preprint. Discussion started: 8 April 2025

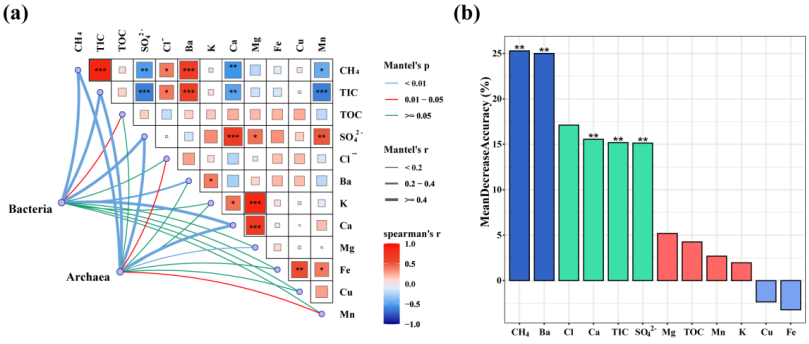

752

753 Fig. 4. Horizontal environmental heterogeneity leads to prokaryotic community
754 diversity: (a) Mantel test for analyzing the correlation between environmental
755 parameters and community composition of prokaryotes; (b) Random Forest mean
756 predictions of the impact of environmental variables on different sites. Note: TIC, total
757 inorganic carbon; TOC, total organic carbon.

758

https://doi.org/10.5194/egusphere-2025-1372
Preprint. Discussion started: 8 April 2025

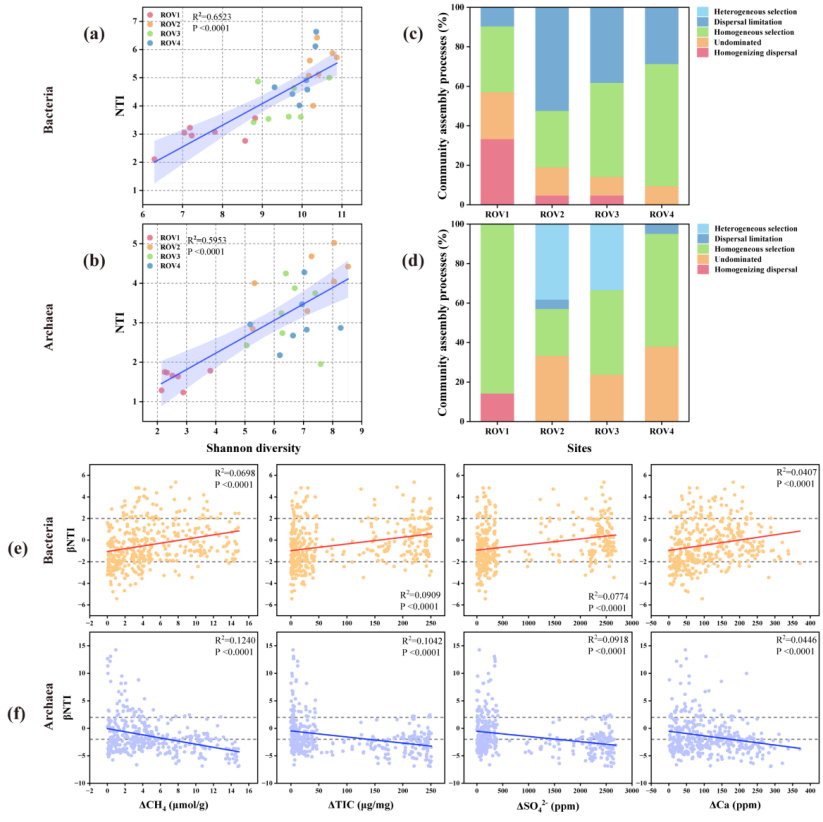

Fig. 5. Community assembly mechanism of bacteria and archaea along the horizontal dimension for the sites ROV1, ROV2, ROV3, and ROV4: variation of (a) bacterial and (b) archaeal community nearest-taxon index (NTI) with the Shannon index; (c) bacterial and (d) archaeal community assembly mechanism at different sites; variation of β-NTI in (e) bacterial and (f) archaeal communities with environmental factors. Note: TIC, total inorganic carbon.

https://doi.org/10.5194/egusphere-2025-1372
Preprint. Discussion started: 8 April 2025

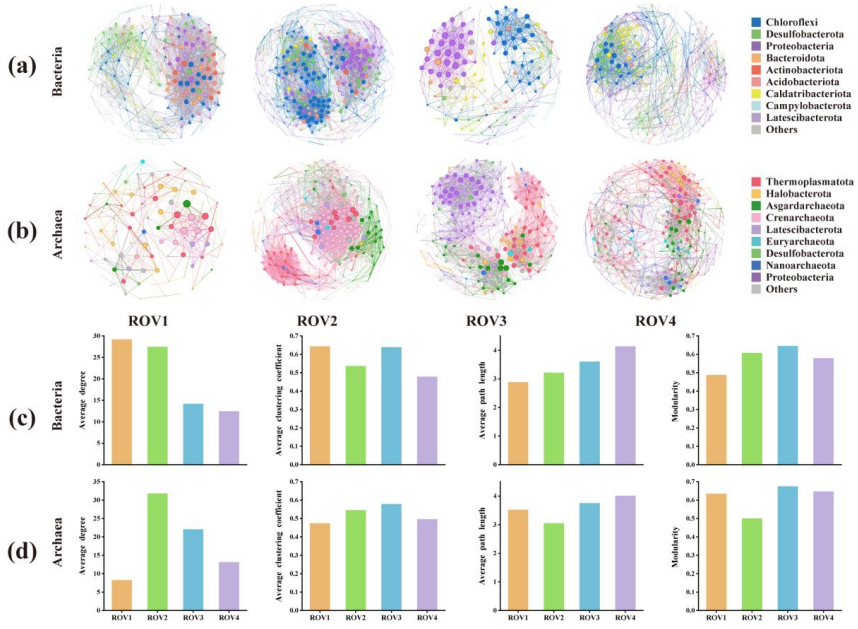

Fig. 6. Phylum level microbial co-occurrence networks at sites ROV1, ROV2, ROV3, and ROV4 and links of topological parameters with sites; phylum level co-occurrence networks of (a) bacterial and (b) archaea communities at different sites. Different colors represent different phyla, lines represent connections between microbes, and node sizes represent the proportion of operational taxonomic units of the phylum; network topological parameters (average degree, average clustering coefficient, average path length and modularity) of co-occurrence of (c) bacterial and (d) archaea communities at different sites.